Discrete-Time ESO for the Disturbance Estimation in the Position Control of a PMSM Drive

Conference Paper · November 2022

DOI: 10.1109/COMRob57154.2022.9962263

4 authors, including:

Omar sandre hernandez
Consejo Nacional de Ciencia y Tecnología
29 PUBLICATIONS **239** CITATIONS

SEE PROFILE

Roberto Morales-Caporal
Instituto Tecnológico de Apizaco
136 PUBLICATIONS **1,133** CITATIONS

SEE PROFILE

P. Ordaz
Autonomous University of Hidalgo
65 PUBLICATIONS **417** CITATIONS

SEE PROFILE

Discrete-Time ESO for the Disturbance Estimation in the Position Control of a PMSM Drive

1st O. Sandre Hernandez
ICBI - AACyE
UAEH - CONACyT
Hidalgo, Mexico
omar_sandre@uaeh.edu.mx

2nd R. Morales Caporal
Postgraduate Studies and Research Division
Technological Institute of Apizazo
Tlaxcala, Mexico
rmcaporal@hotmail.com

3rd P. Ordaz-Oliver
ICBI-AACyE
UAEH
Hidalgo, Mexico
jesus_ordaz@uaeh.edu.mx

4th F. Gonzalez Saenz
ICBI - AACyE
UAEH
Hidalgo, Mexico
fbsaenz095@gmail.com

***Abstract*—This paper presents a discrete-time extended state observer (ESO) for the disturbance estimation in the integral state feedback position control of a permanent magnet synchronous motor (PMSM) drive. First, the system model and the state feedback control are introduced. Next, a discrete-time ESO is formulated for both the state and the disturbance estimation. The disturbance estimation is used actively to compensate for the lumped disturbance in the position control of the PMSM drive. Simulation results are presented to evaluate the proposed methodology. The results demonstrate that mismatched disturbances can be mitigated by the application of the proposed discrete-time ESO.**

***Index Terms*—disturbance rejection, position control, ESO, PMSM**

I. Introduction

The permanent magnet synchronous motor (PMSM) is highly used in applications of motion control due to characteristics like a fast dynamic response, low inertia, and high power density [1]. For many industrial applications like robotics, computer-controlled machines, or machine tools, a high-performance controller is needed to regulate the dynamic response of the PMSM. One of the most popular control schemes for PMSM drives is the field-oriented control (FOC) [2]. In the FOC, the direct d and the quadrature q currents of the PMSM are controlled separately, commonly with a proportional-integral (PI) controller. The application of FOC results in the indirect control of the flux and torque of the PMSM. Typically, an outer loop is used for the regulation of the speed and position of the machine.

The outer loop can be designed based on different control approaches, for instance, model predictive control [3], sliding mode control [4], backstepping control [5], fuzzy control [6], adaptive control [7], and state feedback control [8], [9]. Regardless of the control strategy used for the outer loop design, the control objective is to reject disturbances in the speed or position of the machine. These disturbances are commonly associated with internal uncertainties and external perturbations, however, in this paper both uncertainties and perturbations are considered as a lumped disturbance.

To mitigate the effect of the lumped disturbance in the dynamic response of a system, the control design is commonly treated as a robustness problem, which is a significant research area in modern control theory. On the other hand, the problem of lumped disturbance is also approached as a disturbance rejection control, where, the term rejection is synonymous with attenuation, mitigation, or compensation [10]. In this approach, the control design is simplified, as the idea behind is that a full model of the controlled system is not needed. Hence, the model of the controlled system is divided into the linear part and the lumped disturbance. And it is considered that the lumped disturbance includes nonlinear terms, internal uncertainties, and external perturbations. The idea is to use the theory of linear systems for the control design of the linear part of the system; and to estimate, based on an extended state-observer (ESO), the lumped disturbance to actively reject it [11].

Disturbance rejection has been applied in the control of the PMSM. For instance, in [12] an exponential ESO is used to mitigate the effects of the perturbation in the predictive current control of the PMSM. In [13], the application of the Kalman filter with the moving horizon estimator for the robust predictive current control of a PMSM is presented. In [14], a linear ESO for the current control of the PMSM is presented, in this paper the model is rewritten as a chain of integrators for the observer design. In [5], a non-linear disturbance observer based on backstepping control is presented for the position control of a PMSM. The aforementioned methods will rely in complex control schemes, however, simple controllers like state-feedback control are a possibility for the disturbance rejection in the control of a PMSM.

In this paper, the design and application of a discrete-time ESO (DESO) based integral state feedback control (I-SFC) is proposed. The presented DESO-based I-SFC is based on [10] and it is further extended to discrete-time domain. The I-SFC is used to regulate the angular position of the PMSM, while the DESO is used to estimate the lumped disturbance in the drive. The control and observer design is based on the theory of linear system, making the control design relatively simple. The estimated lumped disturbance is used to attenuate the effects of the real perturbation of the system. The control scheme results in a state-feedback control with active disturbance rejection capabilities. To evaluate the response of the propose methodology, simulation results of a PMSM drive in Matlab/Simulink are presented.

II. Theoretical Background

A. System Model

The PMSM in the $d-q$ reference frame can be described by the combination of the electrical and the mechanical model. Thus, the voltage equations of the PMSM are given by [1]:

$$\dot{\mathbf{x}}^{dq}(t) = \mathbf{A}^{dq}\mathbf{x}^{dq}(t) + \mathbf{B}^{dq}\mathbf{u}^{dq}(t) + \mathbf{B_v}^{dq}, \tag{1}$$

where

$$\mathbf{A}^{dq} = \begin{bmatrix} -\frac{R_s}{L_{sd}} & p\omega_m(t) \\ -p\omega_m(t) & -\frac{R_s}{L_{sq}} \end{bmatrix}, \quad \mathbf{B}^{dq} = \begin{bmatrix} \frac{1}{L_{sd}} & 0 \\ 0 & \frac{1}{L_{sq}} \end{bmatrix},$$

$$\mathbf{x}^{dq}(t) = \begin{bmatrix} i_d \\ i_q \end{bmatrix}, \mathbf{u}^{dq}(t) = \begin{bmatrix} u_d \\ u_q \end{bmatrix}, \mathbf{B}_v^{dq} = \begin{bmatrix} 0 \\ \frac{-p\omega_m(t)\psi_{PM}}{L_{sq}} \end{bmatrix},$$

where L_{sd} and L_{sq} are the inductances in $d-q$ respectively; i_d and i_q are $d-q$ currents; ψ_{PM} is the permanent magnet flux of the rotor; R_s is the stator resistance; ω_m is the mechanical speed; and u_d, u_q are the $d-q$ voltages. For a surface PMSM, it is considered that $L_{sd} = L_{sq} = L_s$, and the following equation describes the electromagnetic torque M_e:

$$M_e = \tfrac{3}{2}p\psi_{PM}i_q = K_T i_q, \tag{2}$$

where p is the pair of poles and $K_T = \frac{3}{2}p\psi_{PM}$. The mechanical model is given by

$$\dot{\mathbf{x}}^{m}(t) = \mathbf{A}^{m}\mathbf{x}^{m}(t) + \mathbf{B}^{m}u^{m}(t) + \mathbf{B_d}^{m}w(t), \tag{3}$$

where

$$\mathbf{A}^{m} = \begin{bmatrix} 0 & 1 \\ 0 & B_m/J \end{bmatrix}, \quad \mathbf{B}^{m} = \begin{bmatrix} 0 \\ \frac{K_T}{J} \end{bmatrix}, \mathbf{x}^{m}(t) = \begin{bmatrix} \theta_m \\ \omega_m \end{bmatrix}$$

$$u^{m}(t) = \begin{bmatrix} i_q \end{bmatrix}, \mathbf{B_d}^{m} = \begin{bmatrix} 0 \\ 1 \end{bmatrix}, w(t) = -\frac{T_L}{J}$$

where θ_m is the mechanical angular position; J is the rotor inertia; M_L is load torque; and B_m is damping coefficient.

B. Field Oriented Control of the PMSM

The control of the PMSM is based on the FOC control scheme. In FOC, an inner loop is used for the current control; and an outer loop for the position/speed control. Conventionally, two PI controllers are used to regulate the i_{dq} currents of the machine, resulting in the indirect control of the flux and torque of the PMSM. After decoupling the current model, the current PI controllers can be designed based on the desired bandwidth as in [15].

The position control is designed in discrete-time, then, (3) is discretized by the application of the Forward Euler method. Since the perturbation $w(t)$ in (3) is unknown, it is not included in the control design, then, the discrete-time model is given by:

$$\begin{aligned} \mathbf{x}(k+1) &= \mathbf{G}\mathbf{x}(k) + \mathbf{H}u(k), \\ y(k) &= \mathbf{C}\mathbf{x}(k), \end{aligned} \tag{4}$$

where $\mathbf{G} = \mathbf{I} + \mathbf{A}^m T_s$; $\mathbf{H} = \mathbf{B}^m T_s$; $\mathbf{C} = [1 \quad 0]$; and T_s is the sampling time. To control (4), an integral state feedback control is used, then the control input $u(k)$ is given by:

$$\begin{aligned} u(k) &= -\mathbf{K}_2\mathbf{x}(k) + K_1 v(k), \\ v(k) &= v(k-1) + r(k) - y(k), \end{aligned} \tag{5}$$

where $\mathbf{K}_2 = [K_{x1} \quad K_{x2}]^T$ is the feedback gain; K_1 is the integral gain; $v(k)$ is the integral error; and $r(k)$ is the desired reference position. Under steady state, and with the appropriate selection of $\mathbf{K}_2$ and K_1; $\mathbf{x}(k)$, $u(k)$, and $r(k)$ will be constant, that is, $\mathbf{x}(\infty)$, $u(\infty)$, and $r(\infty)$ will represent the constant value of the state, the control, and the reference respectively.

Under steady state, the following close loop system is obtained [16]:

$$\zeta(k+1) = \hat{\mathbf{K}}\zeta(k) \tag{6}$$

where

$$\zeta(k) = \begin{bmatrix} \mathbf{x}_e(k) \\ u_e(k) \end{bmatrix} = \begin{bmatrix} \mathbf{x}(k) - \mathbf{x}(\infty) \\ u(k) - u(\infty) \end{bmatrix}$$

$$\hat{\mathbf{K}} = \begin{bmatrix} \mathbf{G} & \mathbf{H} \\ \mathbf{K}_2 - \mathbf{K}_2\mathbf{G} - K_1\mathbf{C}\mathbf{G} & \mathbf{I}_m - \mathbf{K}_2\mathbf{H} - K_1\mathbf{C}\mathbf{H} \end{bmatrix}$$

The dynamic response of (6) will depend on the eigenvalues of $\hat{\mathbf{K}}$. Therefore, the correct selection of the feedback and the integral gain is necessary. Hence, $\mathbf{K_2}$, and K_1 can be designed via pole assignment.

III. Discrete-Time Extended State Observer

The proposed discrete-time extended state observer (DESO) is based on the work presented in [10], and with combination of the composite control law given by (5). For the DESO design, system (3) is now considered with the inclusion of the lumped disturbances. A discrete-time equivalent model of (3) can be obtained as:

$$\begin{aligned} \mathbf{x}(k+1) &= \mathbf{G}\mathbf{x}(k) + \mathbf{H}u(k) + \mathbf{D}f(\mathbf{x}(k), w(k), k), \\ y(k) &= \mathbf{C}\mathbf{x}(k), \end{aligned} \tag{7}$$

where $f(\mathbf{x}(k), w(k), k)$ is the total lumped disturbance that may include external perturbations and unmodeled dynamics. The lumped disturbance is unknown, however, it can be estimated based on the input and output information of (7) by the application of a state observer. To achieve the aforementioned, the lumped disturbance can be considered as an extended state, thus, by defining the lumped disturbance as an augmented variable:

$$x_{n+1}(k) = d(k) = f(\mathbf{x}(k), w(k), k), \tag{8}$$

system (7) can be linearized by the combination of (7) and (8). The extended system equation is obtained as:

$$\begin{aligned} \bar{\mathbf{x}}(k+1) &= \bar{\mathbf{G}}\bar{\mathbf{x}}(k) + \bar{\mathbf{H}}u(k) + \mathbf{E}\Delta d(k), \\ y(k) &= \bar{\mathbf{C}}\bar{\mathbf{x}}(k) \end{aligned} \tag{9}$$

where

$$\bar{\mathbf{G}} = \begin{bmatrix} \mathbf{G} & \mathbf{D} \\ \mathbf{0}_{1\text{x}n} & 0 \end{bmatrix}, \quad \bar{\mathbf{H}} = \begin{bmatrix} \mathbf{H} \\ 0 \end{bmatrix}, \quad \mathbf{E} = \begin{bmatrix} \mathbf{0}_{n\text{x}1} \\ 1 \end{bmatrix},$$

$$\bar{\mathbf{x}}(k) = \begin{bmatrix} \mathbf{x}(k) \\ x_{n+1}(k) \end{bmatrix}, \bar{\mathbf{C}} = [\mathbf{C} \quad 0], \Delta d(k) = d(k+1) - d(k),$$

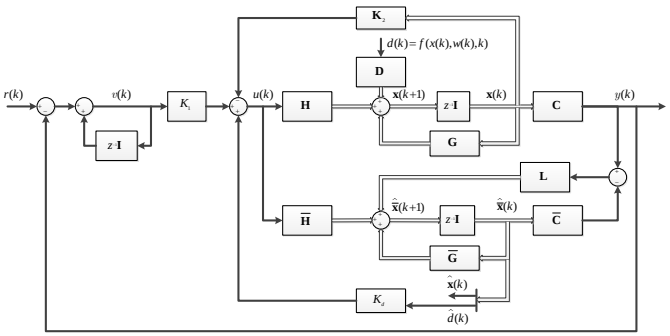

Fig. 1. Simplified block diagram of the DESO-based integral state feedback control.

A. Discrete-time ESO

To design the DESO the following assumptions are made:

- $(\mathbf{G}, \mathbf{H})$ is controllable and $(\mathbf{G}, \mathbf{C})$ is observable
- If $(\mathbf{G}, \mathbf{C})$ is observable, then, $(\bar{\mathbf{G}}, \bar{\mathbf{C}})$ is observable.
- The lumped disturbance $d(k)$ is bounded and slow varying. And $\forall k > 0$, the following holds:

$$|\Delta d(k)| = |d(k+1) - d(k)| < \alpha$$

where α is a constant.

The DESO can be designed based on the classical approach of the Luenberger observer, thus, the DESO is designed as follows:

$$\begin{aligned} \hat{\bar{\mathbf{x}}}(k+1) &= \bar{\mathbf{G}}\hat{\bar{\mathbf{x}}}(k) + \bar{\mathbf{H}}u(k) + \mathbf{L}(y(k) - \hat{y}(k)), \\ \hat{y}(k) &= \bar{\mathbf{C}}\hat{\bar{\mathbf{x}}}(k) \end{aligned} \tag{10}$$

where $\hat{\bar{\mathbf{x}}}(k) = [\hat{\mathbf{x}}(k) \quad \hat{\mathbf{x}}_{n+1}(k)]^T$; and $\hat{\mathbf{x}}(k)$, $\hat{\mathbf{x}}_{n+1}(k) = \hat{d}(k)$, are the estimates of the state variables $\bar{\mathbf{x}}(k)$, $\mathbf{x}(k)$, $\mathbf{x}_{n+1}(k) = d(k)$ respectively; and $\mathbf{L} \in \mathbb{R}^{(n+1)\mathrm{x}1}$ is the observer gain to be designed. For the DESO-based I-SFC, the composite control law is designed as:

$$u(k) = -\mathbf{K}_2\mathbf{x}(k) + K_1 v(k) + K_d\hat{d}(k) \tag{11}$$

where K_d is disturbance compensation gain. Note that in the presence of mismatched uncertainties, the lumped disturbance cannot be eliminated from the state equation since the control input does not have any impact. In the case of mismatched uncertainties, the controller can only mitigate the effect on the output channel. A simplified block diagram of the DESO-based I-SFC is shown in Fig. 1.

B. Stability of the DESO-based integral state feedback control

For simplicity, it is considered that $d(k) = \hat{d}(k)$. Thus, the state and disturbance estimation error, $\mathbf{e}_x$ and e_d respectively, are given by:

$$\begin{aligned} \mathbf{e}_x(k) &= \hat{\mathbf{x}}(k) - \mathbf{x}(k), \\ e_d(k) &= \hat{d}(k) - d(k), \end{aligned} \tag{12}$$

by defining the error variable $\mathbf{e}(k) = [\mathbf{e}_x(k) \quad e_d(k)]^T$, and in combination with (9), (10), and (12), the dynamic error response of the DESO is given by:

$$\mathbf{e}(k+1) = \underbrace{\left(\bar{\mathbf{G}} - \mathbf{L}\bar{\mathbf{C}}\right)}_{\mathbf{G}_e}\mathbf{e}(k) - \mathbf{E}\Delta d(k). \tag{13}$$

The stability of the DESO depends on the selection of the gain observer $\mathbf{L}$. If $\mathbf{L}$ is selected to be make stable $\mathbf{G}_e$, the observer error $\mathbf{e}(k)$ is bounded for a lumped bounded disturbance $\Delta d(k)$. The gain observer $\mathbf{L}$ can be designed via pole assignment, which will result in the bounded-input bounded-output (BIBO) stability of the DESO.

For the system (7), and in combination with the composite control law given by (11), the closed-loop response is given by:

$$\begin{aligned} \mathbf{x}(k+1) = &\overbrace{(\mathbf{G} - \mathbf{H}\mathbf{K}_2)}^{\mathbf{G}_f}\mathbf{x}(k) + \mathbf{H}\bar{\mathbf{K}}\mathbf{e}(k) \\ &+ (\mathbf{D} + \mathbf{H}K_d)\, d(k) + \mathbf{H}K_1 v(k) \end{aligned} \tag{14}$$

where $\bar{\mathbf{K}} = [\mathbf{0}_{1\mathrm{x}n} \quad K_d]$. The closed-loop system given by (14), and the observer error dynamics given by (13), are combined to obtain the closed-loop system of the DESO-based I-SFC. This results in:

$$\begin{aligned} \begin{bmatrix} \mathbf{x}(k+1) \\ \mathbf{e}(k+1) \end{bmatrix} &= \begin{bmatrix} \mathbf{G}_f & \mathbf{H}\bar{\mathbf{K}} \\ \mathbf{0} & \mathbf{G}_e \end{bmatrix} \begin{bmatrix} \mathbf{x}(k) \\ \mathbf{e}(k) \end{bmatrix} \\ &+ \begin{bmatrix} \mathbf{H}K_1 & 0 & \mathbf{D} + \mathbf{H}K_d \\ 0 & -\mathbf{E} & 0 \end{bmatrix} \begin{bmatrix} v(k) \\ \Delta d(k) \\ d(k) \end{bmatrix} \end{aligned} \tag{15}$$

It can be seen from (15) that the dynamic response of the closed-loop system depends on the appropriate selection of the feedback gain $\mathbf{K}_2$ and the gain observer $\mathbf{L}$. If $\mathbf{K}_2$ and $\mathbf{L}$ are designed to make $\mathbf{G}_f$ and $\mathbf{G}_e$ stable respectively, and for any bounded $d(k)$ and $\Delta d(k)$, the closed-loop system of the DESO-based I-SFC is BIBO stable.

To determine the value of K_d, and supposing that $\mathbf{G}_f$ is non-singular, system (14) can be rewritten as

$$\begin{aligned} \mathbf{x}(k) = \mathbf{G}_f^{-1}\Big[&\mathbf{x}(k+1) - \mathbf{H}K_d e_d \\ &- (\mathbf{D} + \mathbf{H}K_d)\, d(k) - \mathbf{H}K_1 v(k)\Big] \end{aligned} \tag{16}$$

by using (16) in the output of system (7), the output can be rewritten as:

$$\begin{aligned} y(k) = \mathbf{C}\Bigg[\mathbf{G}_f^{-1}\Big[&\mathbf{x}(k+1) - \mathbf{H}K_d e_d \\ &- (\mathbf{D} + \mathbf{H}K_d)\, d(k) - \mathbf{H}K_1 v(k)\Big]\Bigg] \end{aligned} \tag{17}$$

It can be seen from (17) that K_d can be selected to attenuate the lumped disturbance in the output of the system. Then, K_d can be selected as:

$$K_d = -\left[\mathbf{C}\mathbf{G}_f^{-1}\mathbf{H}\right]^{-1}\mathbf{C}\mathbf{G}_f^{-1}\mathbf{D} \tag{18}$$

By using (18), (17) is rewritten as:

$$y(k) = \mathbf{C}\mathbf{G}_f^{-1}\mathbf{x}(k+1) - \mathbf{C}\mathbf{G}_f^{-1}\left(\mathbf{D}e_d(k) + \mathbf{H}K_1 v(k)\right) \tag{19}$$

It can be seen that the selection of K_d by (18) results in the theoretical elimination of the lumped disturbance in the output channel, however, this may not be the case in practical engineering. Moreover, as mentioned before, mismatched uncertainties cannot be completely eliminated from the system response.

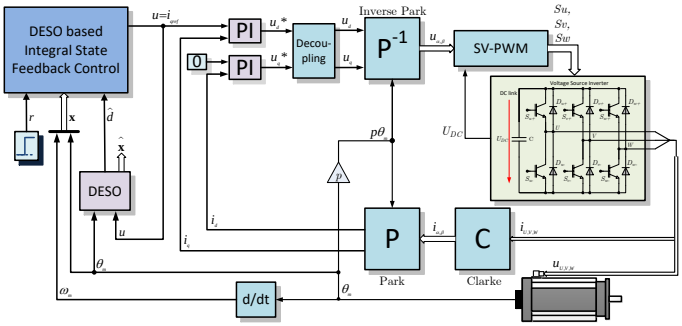

Fig. 2. FOC control scheme with DESO-based integral state feedback control.

TABLE I
MACHINE PARAMETERS

120V, PMSM			
Parameter	**value**	**Parameter**	**value**
T_{LN}	0.32 Nm	p	4
R_s	2.45 Ω	Ω_{nom}	3000 Rpm
L_{sd}	2.95 mH	L_{sq}	2.95 mH
ψ_{PM}	0.024 Vs	i_N	1.65 A rms
J	$42.228 \cdot 10^{-3}$ $kgcm^2$		

C. Considerations for the DESO design

For the DESO-based I-SFC, K_1, $\mathbf{K}_2$, K_d, and $\mathbf{L}$ need to be designed. It can be seen that the DESO error is not reachable from the controller, hence, the I-SFC can be designed separately from the DESO. Both, the controller and the observer can be designed by pole assignment, however, as with any observer-based controller, the dynamic response of the observer needs to be faster than the dynamic response of the controller. Therefore, the poles of the DESO need to be selected for a faster dynamic response than the poles of the controller.

Finally, note the DESO estimates states of the system and the lumped disturbance, hence, the estimates states can be used for the I-SFC. The feedback control using the estimated states results in a similar analysis to the one presented in section B, here omitted due to space. Then, in the case of unmeasurable states, the proposed DESO is still a possibility for a control system.

IV. APPLICATION OF THE DESO IN THE PMSM POSITION CONTROL

In the FOC of the PMSM, electrical and mechanical control can be designed independently. In this section, the mechanical system is considered for the position control of the PMSM. The PMSM under test is an Applied Motion PMSM model j0100-301-3-000 and the parameters are presented in table I. A block diagram of the control scheme is shown in Fig. 2, where the index (k) has been omitted for simplicity.

The general structure of FOC includes two current loop controllers, in this paper the i_d current reference i_{dref} is set to zero to work under the constant torque angle, this results in the direct torque control of the machine based on

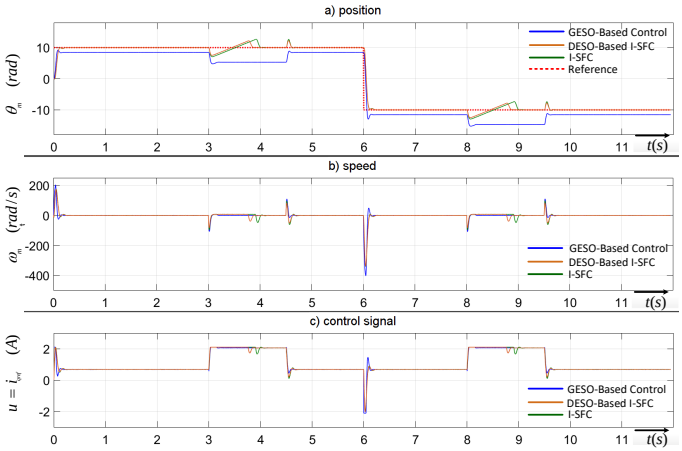

Fig. 3. Reference tracking of step input of the DESO-based I-SFC.

TABLE II
FEEDBACK CONTROL AND DESO GAINS

	Related poles	**Control gains**
I-SFC	$P_1 = 0.9899 + 0.0104i$ $P_2 = 0.9899 - 0.0104i$ $P_3 = 0.9899 + 0.0104i$	$K_1 = 0.004826$ $\mathbf{K}_2 = [0.9396 \quad 0.00689]$
DESO	$P_1 = 0.29$ $P_2 = 0.29$ $P_3 = 0.29$	$\mathbf{L} = \begin{bmatrix} 1.115 \\ 1841.8928 \\ -122.8665 \end{bmatrix}$
$K_d = -0.9166$		

the i_q current. The DESO-based I-SFC is used to regulate the position of the machine. The output of this controller is the i_q current reference i_{qref} for the current control loop. The voltage command is the current controllers output, which is synthesized by the space vector pulse width modulation (SV-PWM) and applied to the machine through a three-phase power inverter.

The simulation of the control scheme shown in Fig. 2 is implemented in Matlab/Simulink. A sampling time of $T_{sc} = 100\mu s$ is used in the current control loop, this results in a switching frequency of $10kHz$ for the power inverter. For the position control loop a sampling time of $T_{sp} = 200\mu s$ is used. System (3) is converted in its equivalent discrete-time model using T_{sp} as mentioned in section 2-B. For the discrete-time system $(\mathbf{G}, \mathbf{H})$ is controllable and $(\mathbf{G}, \mathbf{C})$ is observable. The torque load is considered as the lumped perturbation in the system. The desired poles and the control gains, and the value of K_d according to (18), are listed in table II.

For all simulations the state is considerable to be measurable, as in most applications the PMSM has a position sensor mounted on the shaft. The steady-state and the transient-state is evaluated during the simulations under two different perturbations. The maximum value of T_L is 0.3 Nm as listed in table I, hence, the bound $\alpha = 0.3$. In the first evaluation (case 1) the initial value of $T_L = 0.1Nm$, at 3s $T_L = 0.3Nm$, at 4.5s $T_L = 0.1Nm$, at 8s $T_L = 0.3Nm$, and finally at

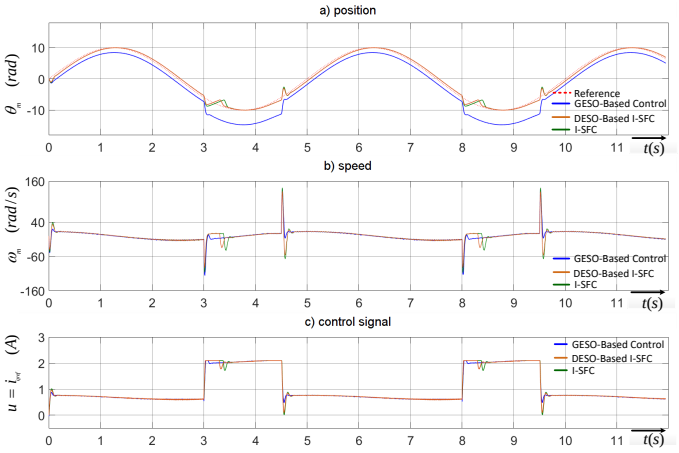

Fig. 4. Reference tracking of sine-wave input of the DESO-based I-SFC.

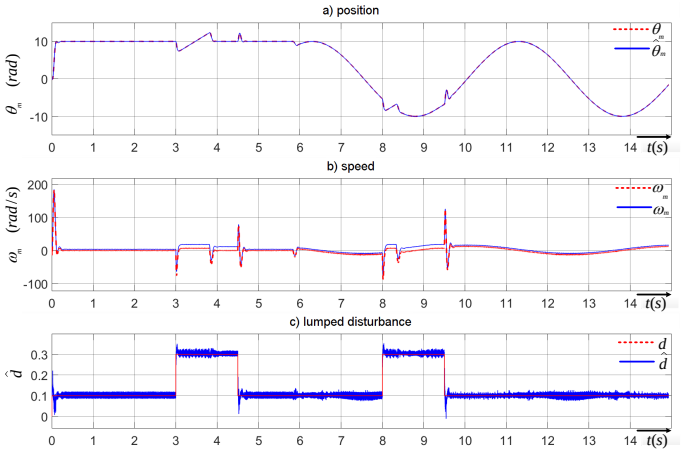

Fig. 6. State and disturbance estimation under step perturbation of the DESO-based I-SFC.

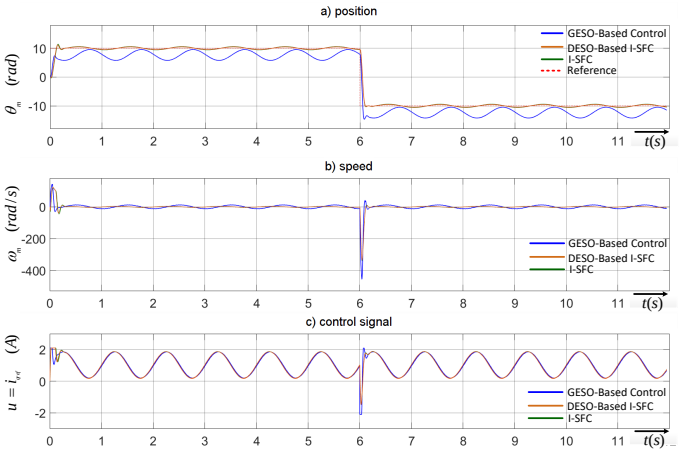

Fig. 5. Reference tracking of step input under sinusoidal perturbation of the DESO-based I-SFC.

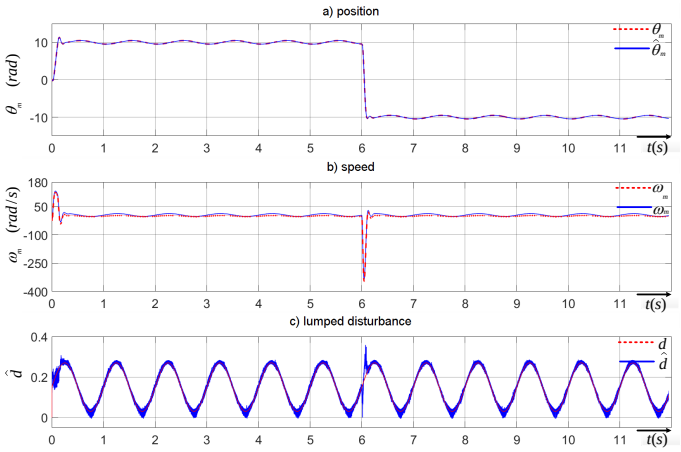

Fig. 7. State and disturbance estimation under sinusoidal perturbation of the DESO-based I-SFC.

9.5s $T_L = 0.1Nm$. In the second evaluation (case 2) the perturbation for the $T_L = 0.12\sin(2\pi) + 0.15$. A comparison with the generalized extended estate observer (GESO) - based control presented in [10] is presented to validate the proposed methodology.

The reference tracking for an step input is shown in Fig.3. In this evaluation the reference position is fixed at the initial time to 10 rad/s, and in the time instant of 6s the reference position is set to -10 rad/s; the case 1 is considered for the perturbation. The simulation results shown reference tracking is performed successfully in the DESO-based I-SFC, and the position of the PMSM follows the reference despite the perturbation. The evaluation of the performance under the I-SFC and the GESO-based control is also evaluated. It can be seen that I-SFC present an slightly larger variance compared to the DESO-based I-SFC. Moreover, the GESO-based control present a significant steady-state error.

The reference tracking for a sine-wave input is shown in Fig 4. In this evaluation the reference position is given by $10\sin(2\pi 0.2)$, while case 1 is considered for the perturbation. The simulation results are similar to the one obtained under the step input reference tracking. In this case, the DESO-based I-SFC presents a better reference tracking behavior than the I-SFC. In the case of the GESO-based control, an steady-state error is presented.

The evaluation of the reference tracking for an step input similar to the one evaluated previously is presented in Fig. 5. In this test the reference position is exactly the same than the previous case, however, case 2 for the perturbation is used. In all controllers, the simulation results show that a significant error is presented during the reference tracking, which presents constants oscillations and the perturbation is not successfully attenuated.

The state estimation is evaluated for case 1 and case 2 of the lumped disturbance. For case 1, the reference position is set to 10 rad/s and at 6 s is set to $10\sin(2\pi 0.2)$. The simulation results are shown in Fig. 6. It can be seen that the position and disturbance are estimated successfully, however, a steady-

state error in the speed estimation is presented. For case 2, the position reference is set to 10 rad/s at 0s, and at 6s the reference position is set to -10 rad/s. The simulation results are shown in Fig. 7. Similar results are obtained for the state and the disturbance estimation. In this test, the position and disturbance are estimated successfully, however, a steady-state error in the speed estimation is presented.

The evaluation results show that the presented DESO can be used to estimate the lumped disturbance of the system, and can be used to design a controller to attenuate it in the output channel. In the case of the GESO-based control, the results show that a steady-state error is always presented in the system. This is attributed to the realization of the GESO as discussed in [17]. An alternative is to design a proportional-integral observer. However, the integrator can be added to the controller as in this paper. Since the DESO is estimating accurately the disturbance, the integrator action can be added in the control action as in the proposed DESO-based I-SFC. This results in the elimination of the steady-state error for constant lumped disturbances. In the case of time-varying disturbance, further research is needed.

V. Conclusions

This paper presents the design of a DESO-based I-SFC ans its application to the position control of a PMSM. The state-observer and control design is performed in discrete-time for its future application in a digital platform. The simulation results show that under constant disturbances the proposed DESO-based I-SFC is able to attenuate the effect of the disturbance in the system, however, is in the presence of time-varying disturbances is not possible to eliminate the effect on the controlled system. Further research is needed to compensate the time-varying disturbances.

References

[1] R. Krishnan, *Permanent magnet synchronous and brushless DC motor drives*. CRC press, 2017.

[2] M. Ahmad, *High performance AC drives: modelling analysis and control*. Springer Science & Business Media, 2010.

[3] S. Vazquez, J. Rodriguez, M. Rivera, L. G. Franquelo, and M. Norambuena, "Model predictive control for power converters and drives: Advances and trends," *IEEE Transactions on Industrial Electronics*, vol. 64, no. 2, pp. 935–947, 2017.

[4] X. Zhang, L. Sun, K. Zhao, and L. Sun, "Nonlinear speed control for pmsm system using sliding-mode control and disturbance compensation techniques," *IEEE Transactions on Power Electronics*, vol. 28, no. 3, pp. 1358–1365, 2013.

[5] L. Li, J. Xiao, Y. Zhao, K. Liu, X. Peng, H. Luan, and K. Li, "Robust position anti-interference control for pmsm servo system with uncertain disturbance," *CES Transactions on Electrical Machines and Systems*, vol. 4, no. 2, pp. 151–160, 2020.

[6] Y.-S. Kung and M.-H. Tsai, "Fpga-based speed control ic for pmsm drive with adaptive fuzzy control," *IEEE Transactions on Power Electronics*, vol. 22, no. 6, pp. 2476–2486, 2007.

[7] Y. A.-R. I. Mohamed and E. F. El-Saadany, "A current control scheme with an adaptive internal model for torque ripple minimization and robust current regulation in pmsm drive systems," *IEEE Transactions on Energy Conversion*, vol. 23, no. 1, pp. 92–100, 2008.

[8] A. Apte, V. A. Joshi, H. Mehta, and R. Walambe, "Disturbance-observer-based sensorless control of pmsm using integral state feedback controller," *IEEE Transactions on Power Electronics*, vol. 35, no. 6, pp. 6082–6090, 2020.

[9] T. Tarczewski and L. M. Grzesiak, "Constrained state feedback speed control of pmsm based on model predictive approach," *IEEE Transactions on Industrial Electronics*, vol. 63, no. 6, pp. 3867–3875, 2016.

[10] Z. Gao, "On the centrality of disturbance rejection in automatic control," *ISA Transactions*, vol. 53, no. 4, pp. 850–857, 2014, disturbance Estimation and Mitigation. [Online]. Available: https://www.sciencedirect.com/science/article/pii/S0019057813001559

[11] S. Li, J. Yang, W.-H. Chen, and X. Chen, "Generalized extended state observer based control for systems with mismatched uncertainties," *IEEE Transactions on Industrial Electronics*, vol. 59, no. 12, pp. 4792–4802, 2012.

[12] F. Wang, D. Ke, X. Yu, and D. Huang, "Enhanced predictive model based deadbeat control for pmsm drives using exponential extended state observer," *IEEE Transactions on Industrial Electronics*, vol. 69, no. 3, pp. 2357–2369, 2022.

[13] X. Li, W. Tian, X. Gao, Q. Yang, and R. Kennel, "A generalized observer-based robust predictive current control strategy for pmsm drive system," *IEEE Transactions on Industrial Electronics*, vol. 69, no. 2, pp. 1322–1332, 2022.

[14] L. Qu, W. Qiao, and L. Qu, "An enhanced linear active disturbance rejection rotor position sensorless control for permanent magnet synchronous motors," *IEEE Transactions on Power Electronics*, vol. 35, no. 6, pp. 6175–6184, 2020.

[15] M. Wishart, G. Diana, and R. Harley, "Controller design for applying field-oriented control to the permanent magnet synchronous machine," *Electric Power Systems Research*, vol. 19, no. 3, pp. 219–227, 1990. [Online]. Available: https://www.sciencedirect.com/science/article/pii/0378779690900352

[16] K. Ogata, *Discrete-time control systems*. Prentice-Hall, Inc., 1995.

[17] S.-K. Kim, "Offset-free one-step ahead state predictor for power electronic applications using robust proportional–integral observer," *IEEE Transactions on Industrial Electronics*, vol. 63, no. 3, pp. 1763–1770, 2016.